Electronic Supplementary Material (ESI) for Lab on a Chip.

Supplementary Information

All-optical tuning of magnetic-fluid-filled optofluidic ring resonator

Yang Liu,[a] Lei Shi,*[a] Xinbiao Xu[a], Ping Zhao,[a] Zheqi Wang,[a] Shengli Pu,[b] and Xinliang Zhang*[a]

[a] Wuhan National Laboratory for Optoelectronics, Huazhong University of Science and Technology, Wuhan 430074, China. E-mail: lshi@mail.hust.edu.cn; xlzhang@mail.hust.edu.cn

[b] College of Science, University of Shanghai for Science and Technology, Shanghai 200093, China.

This Supplementary Information includes:

1. Simulation of the electric field distribution in WGMs (Supplementary Figure S1)
2. Experimental results and calculation for the coupling efficiency (Supplementary Figure S2-3)
3. Transmission spectra of OFRRs before and after the MFfilling (Supplementary Figure S4)
4. Transmission spectra of OFRRs with different power of the broadband source (Supplementary Figure S5)
5. Simulation results of the electric field distribution around the fiber tip (Supplementary Figure S6-7)
6. Optical microscope graphs of the relative positions of the fiber tip and the microcapillary (Supplementary Figure S8)
7. Experimental arrangement for the analysis on the dynamic response of the device (Supplementary Figure S9)
8. Supplementary References

1. Simulation of the electric field distribution in WGMs (Supplementary Figure S1)

In order to provide a better explanation, a 2D simulation was performed to evaluate the electric field distribution of a silica microcapillary in contact with a silica microfiber using commercial finite element method software (COMSOL MULTIPHYSICS 4.3b, Stockholm, Sweden), as shown in Fig. S1(a). It can be seen that the electric field of circulating light mainly distributes near the outer wall of the silica microcapillary, which means that the majority of the resonance wavelength can avoid being absorbed by MF. Therefore, the quality factor would not decrease evidently. But, it is worth mentioning that there is still some light extending towards the inner wall surface, although it is pretty weak, as shown in Fig. S1 (a-b).

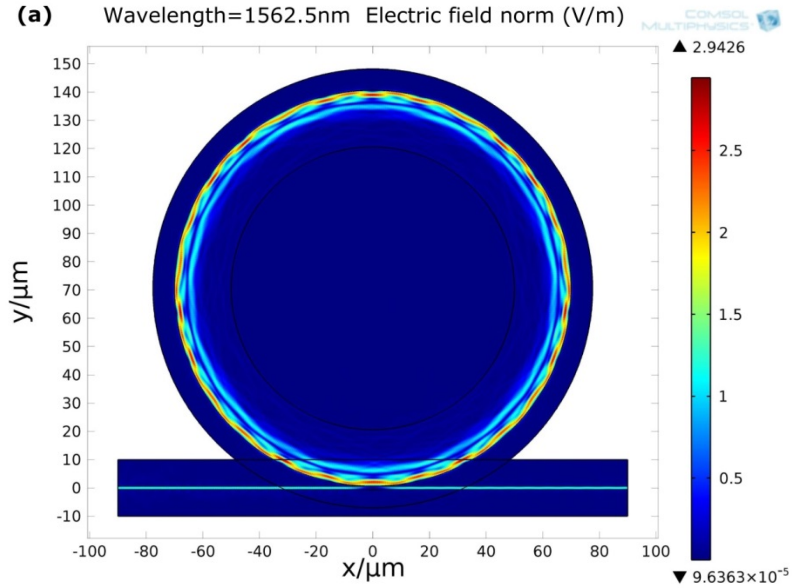

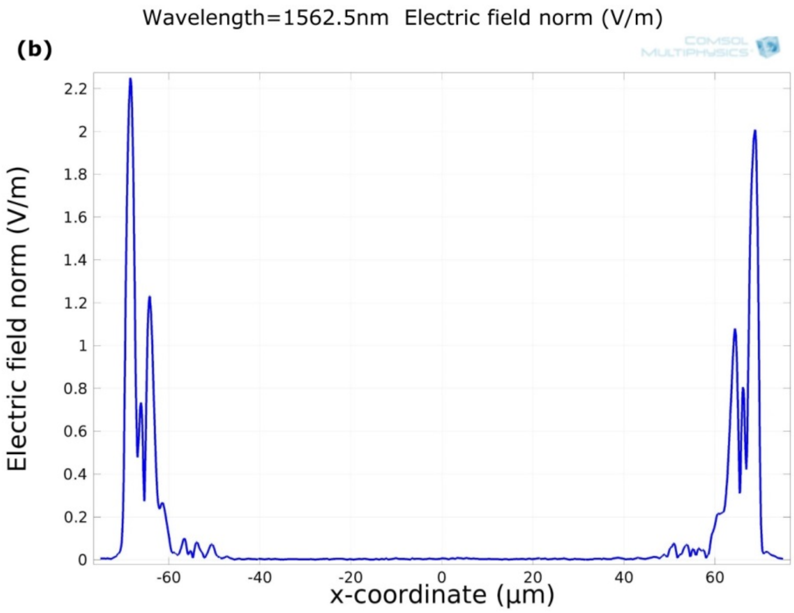

Fig.S1 (a) 2D simulated electric field distribution for a silica microcapillary. λ=1562.5 nm light is coupled into the microcapillary from an adjacent silica microfiber. (b) The field profile is taken along a cut line y=70μm. The inner radius of the microcapillary is 50μm, and the outer radius is 70μm.

2. Experimental results and calculation for the coupling efficiency (Supplementary Figure S2-3)

In order to illustrate how the coupling efficiency affects the transmission spectrum of the device, experiments and calculations were performed. The coupling efficiency between the microcapillary and a microfiber can be enlarged by reducing the diameter of the microfiber and their gap. The coupling efficiency mainly affects extinction ratio, quality factor, and mode numbers of the transmission spectrum, according to equations proposed by B. E. Little *et al.*[1]

We made use of the taper-like profile of a fiber taper during the experiment. We tuned the fiber along its axis orientation, so that we can change the spot where the microfiber taper contacted the microcapillary. This can be treated as that the microcapillary coupled with microfibers with different diameters. As shown in Fig. S2, as the diameter decreases, the coupling efficiency becomes higher because of the larger evanescent field of the microfiber. It can be easily seen that, the rejection ratio of resonance wavelength grows, quality factor drops and higher order modes appears when the coupling efficiency increases. Simultaneously, the power of the transmission spectrum also decreases as the increase in coupling efficiency.

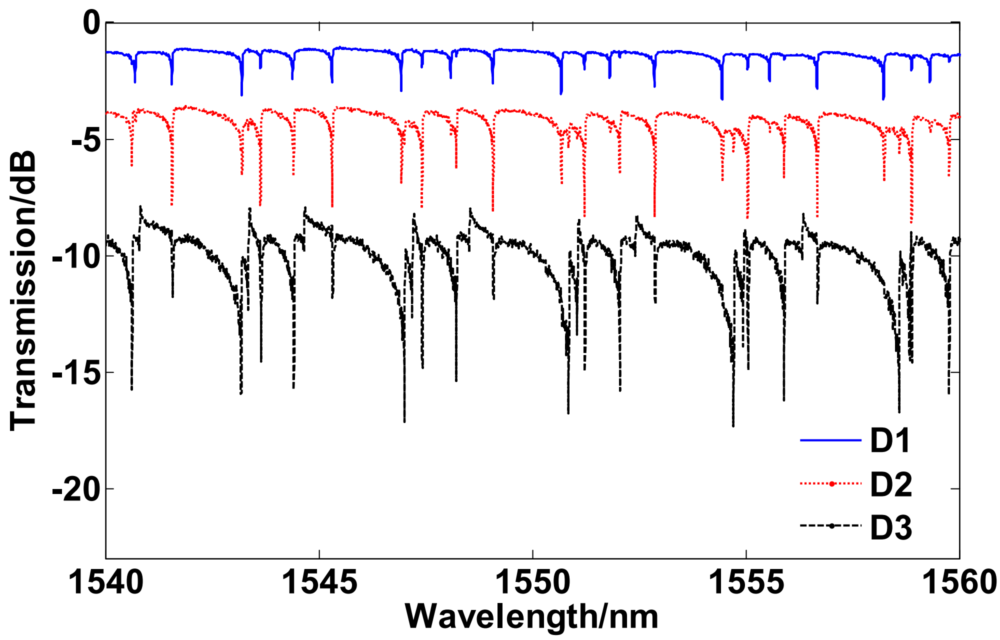

Fig. S2 Transmission spectrum of an air-filled OFRR coupling with a microfiber with different diameters. D1, D2 and D3 represent different diameters, among which D1 is the largest while D3 is the smallest.

Also, the coupling efficiency will be higher through reducing the gap between the microfiber and the micro capillary. A numerical calculation was performed with the help of COMSOL and MATLAB according to the theory presented by Ye Liu *et al*[2], as shown in Fig. S3. It shows the coupling efficiency of two polarized light increases as the gap decrease. We expect that changing the coupling efficiency by varying the gap will affect the transmission spectrum in a similar way as shown in Fig. S2.

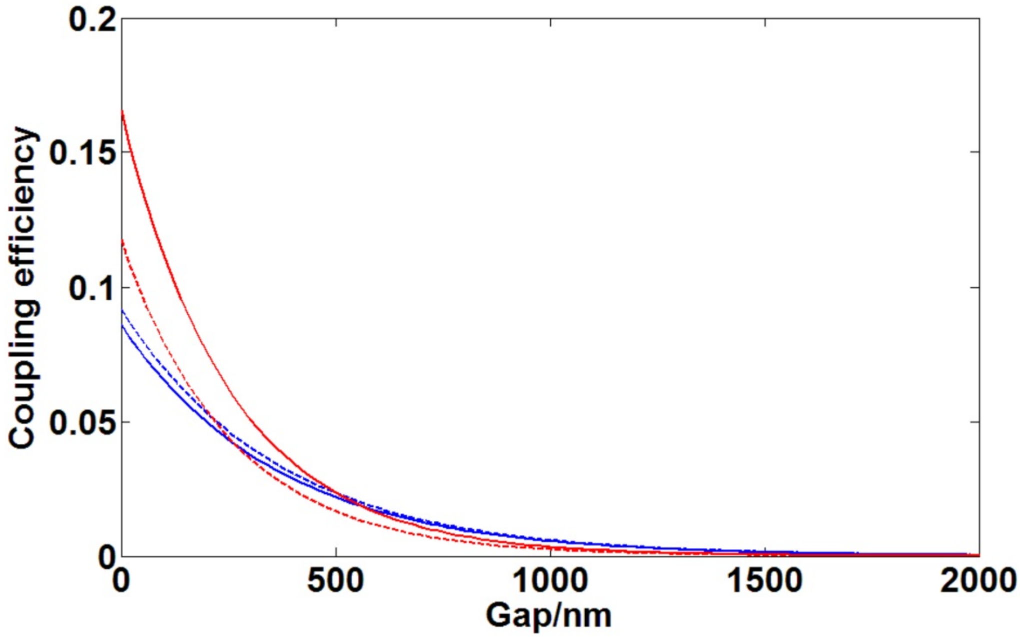

Fig. S3 Coupling coefficiency of TE mode and TM mode in the OFRR with an outer radius of 70μm and an inner radius of 50μm. κ_{12} indicates the coupling efficiency from the microfiber to the microcapillary, while κ_{21} presents the coupling efficiency from the microcapillary to the microfiber.

3. Transmission spectra of OFRRs before and after the MF filling (Supplementary Figure S4)

To verify our theoretical analysis proposed above, comparative experiments were carried out, and the results are presented in Fig. S4. As we know, larger loss will cause evident deterioration of quality factor in a resonator. These results can be thought as a verification which demonstrates that the vast majority of resonance light will not be absorbed by MF due to the relatively thick wall. However, there is still very weak electric field existing around the boundary between MF and the microcapillary.

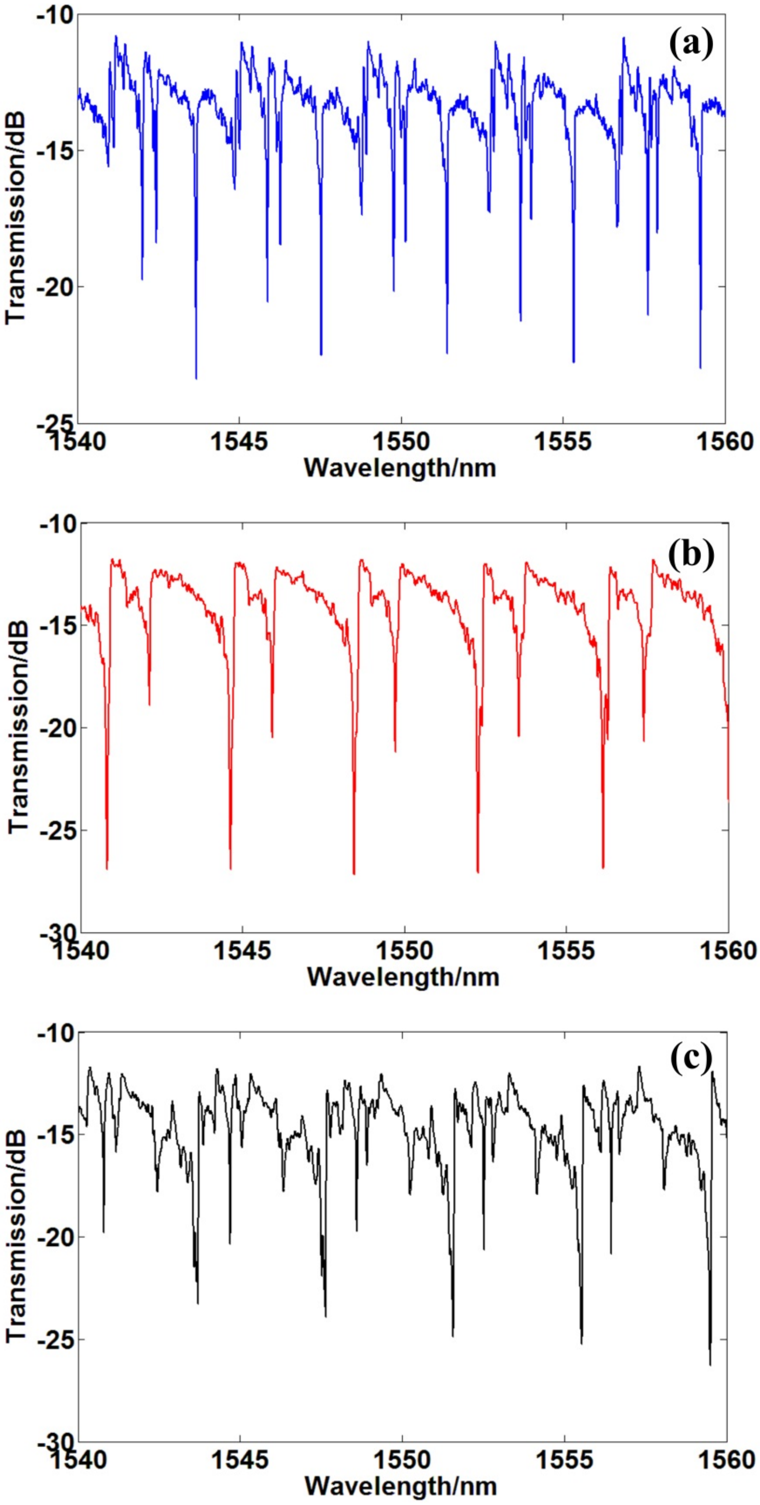

Fig. S4 Transmission spectra of an OFRR before MF filling (a) air, and after (b) water-based MF and (c) kerosene-based MF filling.

4. <u>Transmission spectra of OFRRs with different power of the broadband source (Supplementary Figure S5)</u>

Since there does exist weak absorption of light at resonance wavelength. So quality factor will be affected by light absorption, and the resonance wavelength will shift due to the photothermal effect of MF. To prove this, experiments were carried out. With different liquids filled into the microcapillary, transmission spectra were recorded by an optical spectrum analyzer (OSA) under different power of the broadband source, through tuning a variable optical attenuator (ATT), as shown in Fig. S5. Before testing the OFRR filled with MF, we performed a contrast experiment by filling ethanol which is also a liquid but it is transparent to light, as shown in Fig. S5 (a).

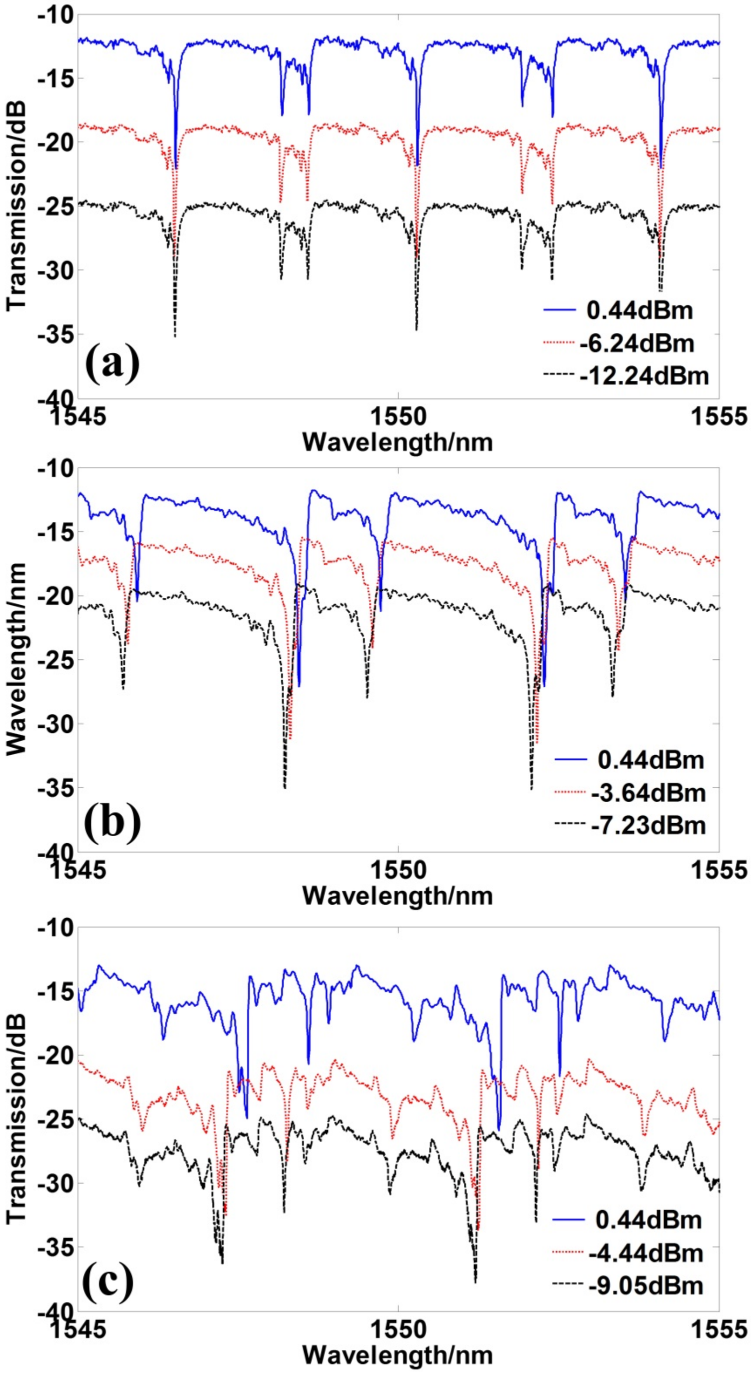

Fig. S5 Transmission spectra of an OFRR under different powers of the broadband source. The OFRR was filled with (a) ethanol, (b) water-based MF and (c) kerosene-based MF, respectively.

5. Simulation results of the electric field distribution around the fiber tip (Supplementary Figure S6-7)

In order to analyzed the temperature distribution around the fiberi tip, simulations and calculations were performed. Due to its axisymmetric structure, a simplified 2D simulation was performed to evaluate the optical electric field distribution of a fiber tip using commercial finite difference time domain software (FDTD solutions, Canada), as shown in Fig. S6. The electric field density becomes larger with the decrease in taper diameter, and then the light is emitted from the tip end where the electric field density is the highest. Apart from that, there exists evident evanescent field out of the taper profile along the taper from Z=1950μm to Z=2000μm. Meanwhile, Fig. S7 shows the electric field distribution along cut lines of the taper cross sections at different taper length Z. Therefore, the electric field is expected to possess an intensity gradient around the fiber in axial and radial direction while a uniform distribution in angular orientation because of tis axisymmetric structure, and it is mainly concentrated around the tip end. Assuming iron oxide nanoparticles dispersing homogeneously, it can be predicted that the temperature will possess a gradient distribution around the fiber tip, analogous to the gradient distribution of electric field.

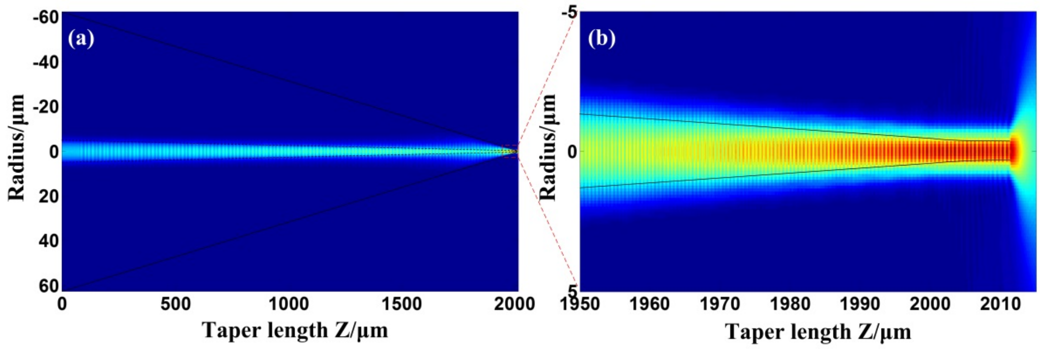

Fig. S6 Electric field distribution of a continuous wave at 1550nm when travelling through a fiber tip along taper length Z. (a) the whole fiber tip with a typical length of 2000μm, evolving from a standard single mode fiber at Z=0. (b) magnification of the tip end which is labelled in (a) .

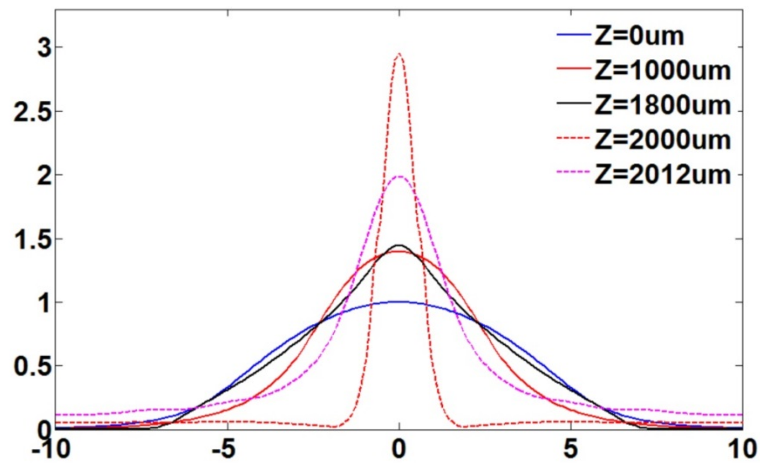

Fig. S7 Electric field distribution along cut lines of taper cross sections at different taper length Z which is presented as the horizontal axis in Fig. S6.

6. Optical microscope graphs of the relative positions of the fiber tip and the

microcapillary (Supplementary Figure S8)

The coupling fiber was moved to a spot where the coupling fiber was the closest to the fiber tip by observing them with an optical microscope, as shown in Fig. S8. The profile of the fiber tip can be clearly distinguished through the optical microscope graph which is helpful for alignment.

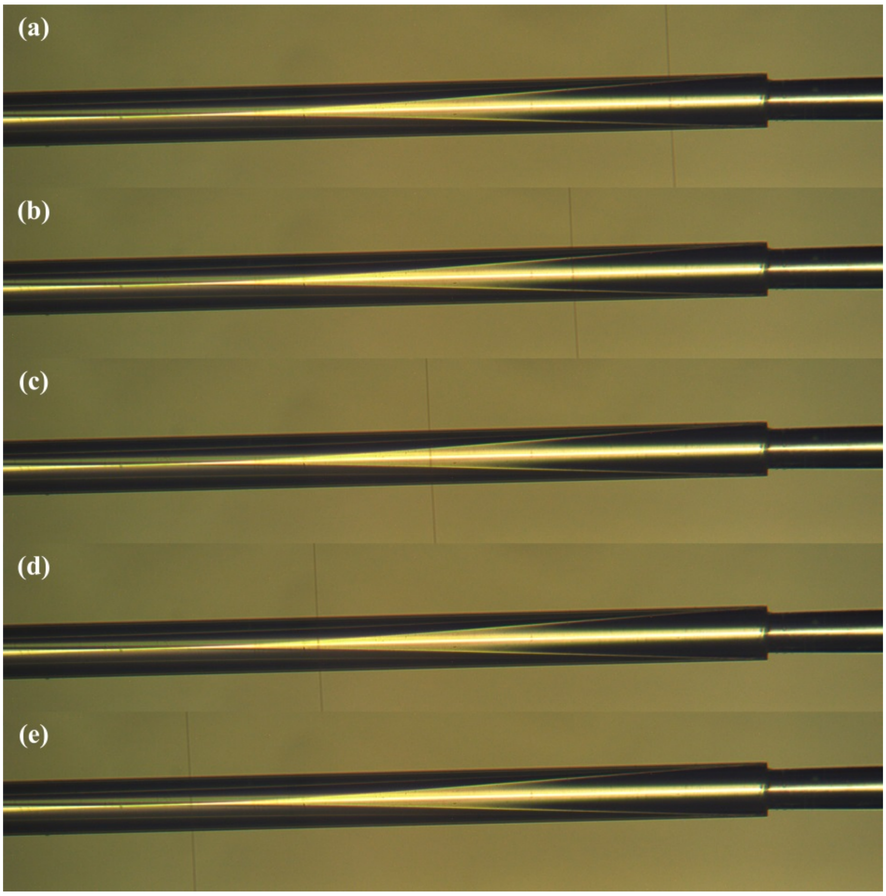

Fig. S8 Optical microscope graphs of a non-filled OFRR with different relatively positions between the coupling fiber and the fiber tip.

7. Experimental arrangement for the analysis on the dynamic response of the device (Supplementary Figure S9)

Experiments were carried out to analyze the dynamic response of the device. Fig. S9 schematically illustrates the experimental setup. A continuous wave (CW) signal generated by a tunable laser diode was used as a pump source. An InGaAs photon diode (PD, DET01CFC, THORLABS) and a digital storage oscilloscope (DSO, DSO7054A, Agilent) were used to detect the transmission power of the light from LD2.

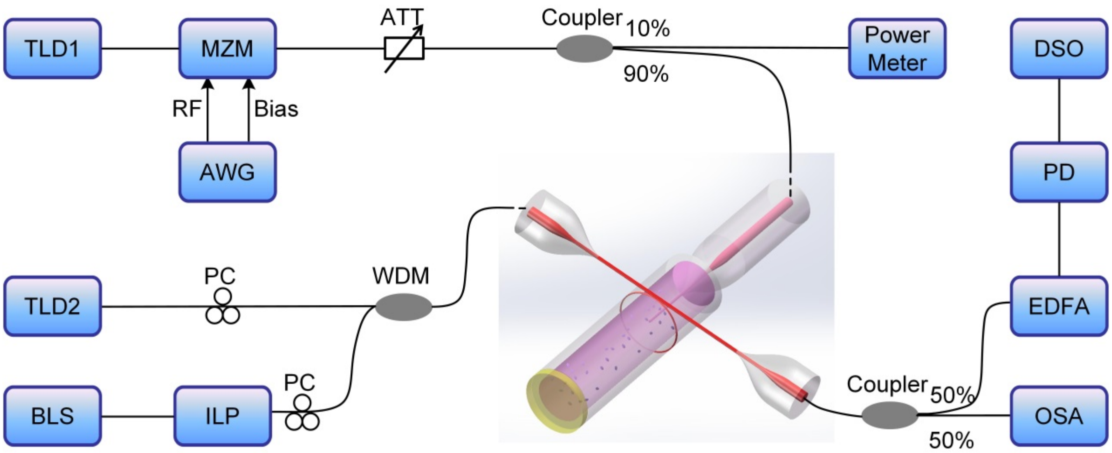

Fig. S9 Experimental setup for tuning properties testing of the AOTOFRR. LD, laser diode. EDFA, erbium-doped fiber amplifier. ATT, variable optical attenuator. BLS, broadband light source. ILP, in-line polarizer. WDM, wavelength division multiplexer. PC, polarization controller. OSA, optical spectrum analyzer. PD, photon diode. DSO, digital storage oscilloscope.

8. Supplementary References

1 Little, B. E., Chu, S. T., Haus, H. A., Foresi, J. & Laine, J. P. Microring resonator channel dropping filters. *Lightwave Technology, Journal of* **15**, 998-1005, doi:10.1109/50.588673 (1997).

2 Liu, Y., Chang, T. & Craig, A. E. Coupled mode theory for modeling microring resonators. *Optical Engineering* **44**, 084601-084601-084606, doi:10.1117/1.2012503 (2005).